*07*

# Micromagnetic simulation of a „majority" logic gate based on the interference of spin waves' caustics

© G.M. Dudko,[1] A.V. Kozhevnikov,[1] V.K. Sakharov,[1] M.E. Seleznev,[1] Y.V. Khivintsev,[1]
   Y.V. Nikulin,[1] S.L. Vysotskii,[1] Y.A. Filimonov,[1] S.A. Nikitov,[2] A. Khitun[3]

[1] Saratov Branch, Kotel'nikov Institute of Radio Engineering and Electronics, Russian Academy of Sciences,
410019 Saratov, Russia
[2] Kotelnikov Institute of Radio Engineering and Electronics, Russian Academy of Sciences,
125009 Moscow, Russia
[3] Electrical Engineering Department, University of California — Riverside,
92521 Riverside, CA, USA

e-mail: yuri.a.filimonov@gmail.com

Using micromagnetic simulations, we show the possibility to build spin logic devices based on films of yttrium iron garnet and permalloy where energy channeling of spin waves is achieved due to excitation of focused and narrow-directed wave beams by used antennas. We studied the methods to construct a „majority" logic gate based on the interference of caustics of spin waves excited by the rectilinear transducers directed at an angle to the in-plane magnetic field. We propose an approach when adding a reference signal with fixed initial phase to three information signals allows to use an amplitude detector at the output of the device to built a truth table. The possibility to scale the device on the example of its work in the range of spin waves with micron and submicron wavelengths is demonstrated.

**Keywords:** spin waves, magnetic field, ferromagnetic films, permalloy.

## Introduction

The effects of propagation and interference of spin waves (SW) in magnetic microstructures are promising for building energy-efficient information technologies based on them [1,2]. A number of prototypes of information processing devices and spin logic based on the interference effects for SW propagating in structures based on waveguides with finite width [1–7] of the order of units of millimeters were proposed.

The current trend in the development of SW devices and their ability to compete with CMOS technologies implies a reduction in the lateral dimensions of the elements to micron and submicron values, however, losses on excitation, propagation and reception of SW [8–10] significantly increase. This is because of the complication of the SW spectrum due to its lateral quantization [11], as well as the growing influence of exchange interaction and demagnetization fields [12], on the one hand, and the influence of technological factors on the parameters of microwaveguides [13], on the other. In addition, in the junctions of magnonic networks based on microwaveguides, there is a redistribution of SW power, which significantly changes the ratio of amplitudes at the output antennas [14]. One of the possible approaches to eliminate the influence of these factors may be the changeover to integrated spin logic devices based on ferromagnetic films, in which the channeling of the SW energy is achieved not due to

their propagation in width-limited waveguides, but due to excitation by antennas that provide the formation of focused or narrowly directed SW beams [15–18]. The purpose of this paper is to show that such an approach can be used as the basis for the operation of the logical „majority" gate.

We note that the majority element (majority gate) this is a logic element from the threshold class [19] with an even or odd number of inputs and one output signal, the value of which coincides with the value on most inputs. If most of the inputs have a signal equivalent to the logical „1" (or „0"), then the output signal will be set to „1" or „0". Majority gates based on spin waves are of particular interest because a simple spin wave adder replaces several dozen transistors, and three majority gates are enough to create a complete adder [20,21]. In addition, the SW majority gate potentially allows parallel data processing in multi-frequency mode [22].

To date, several prototypes of the spin wave majority logic elements where the SW phase was as the logical „1" and „0" have been considered [1,2,23–29]. Prototypes of the majority gate based on normally [27] and tangentially [28] magnetized Ψ-shaped millimeter-sized waveguides made of of yttrium iron garnet (YIG) films with three input and one output SW transducers at the ends were considered. In the study [29], a compact design of the majority gate was proposed based on a micron-sized film waveguide from CoFeB, where the SW transducers were placed along the waveguide axis. In all cases it was assumed that with

attenuators and phase shifters installed in front of the input antennas make possible to provide SW interference with the same wavelengths $\lambda$ and amplitudes, as well as the phase ratio that are necessary for constructive and destructive interference at the output transducer. The output signal was processed by a phase-sensitive detector [28,29], due to which the phase of the output wave is extracted from measurements in the time domain and used to compile a complete table of the truth of the majority function. In this paper, the possibility of constructing a „majority" gate based on the interference of SW caustics formed in a tangentially magnetized ferromagnetic film by SW antennas is investigated using micromagentic simulation. We also show that adding an extra reference signal with a fixed phase „0" or „$\pi$" and a certain amplitude level to the proposed construction of the „majority" gate makes it possible to use an amplitude detector at the output to compile a truth table.

# 1.  Results of micromagnetic simulation

We will consider the majority element based on the SW, schematically shown in Fig. 1, $a$. As a waveguide of the SW medium, we will consider a ferromagnetic film $1$ magnetized by the field $\mathbf{H}$ lying in the plane of the film. The input $2-5$ and output $6$ antennas are located on the surface of the film. We assume that the centers of the input antennas SW are located at the vertices of a rectangle with dimensions $a \times b$ at some angles $\pm\varphi$ with respect to the field $\mathbf{H}$, which provides [15–18] propagation of SW beams $7-10$ at some fixed frequency $f$ in the form of caustics whose group velocity coincides with the direction of the diagonals of the rectangle. The center of the output antenna is located at the intersection of the diagonals, and the output antenna itself is oriented either parallel or perpendicular to the direction of the magnetic field. To simulate the propagation and interference of the SW beams in the structure, the OOMMF [30] package was used. It was assumed that the excitation of the SW is carried out by a field $h_z(t)$ directed along the $Oz$ axis, localized under the input antenna and homogeneous across the film thickness:  $h_z(t) = h_z \cdot \sin(2\pi f t + \varphi_0)$, where $h_z$ — the amplitude of the exciting magnetic field, $f$ — the frequency of the microwave signal; $t$ — the current time; $\varphi_0$ — the initial phase of the input signal. Two-dimensional maps of the Fourier distribution- of the amplitude of the SW field were calculated, as a characteristic of which the microwave magnetization component $m_z$ was taken. The maps were obtained using the Semargl program [31] by processing a time sample of data $m_z(x, y, z, t_i)$ with time increments of 0.1 ns, where the sampling duration depended on the time of the SW travel through the film and ranged from 8 to 100 ns.

Note that the characteristics of the SW caustics are significantly determined by the magnitude of the field $\mathbf{H}$ and the value of the SW frequency, as well as the thickness $d$, the relaxation rate $\alpha$ and magnetization of $4\pi M$ ferromagnetic

film [15–18]. In order to show the possibilities of scaling the proposed approach to the submicron wavelength region we refer to the cases of YIG films with a thickness of $3.9\,\mu\mathrm{m}$ and $50\,\mathrm{nm}$, as well as Permalloy (Pu) films with $d = 100\,\mathrm{nm}$.

## 1.1.  The case of YIG films of micron thicknesses

Let's first consider the interference of caustics in the YIG film with parameters $d = 3.9\,\mu\mathrm{m}$, $4\pi M = 1750\,\mathrm{G}$, exchange stiffness $A = 3.5 \cdot 10^{-12}$ J/m, $\alpha = 10^{-3}$, the gyromagnetic ratio $\gamma = 2.8$ GHz/kOe and with planar dimensions of $1.5 \times 1.5$ mm, for which the SW interference can be experimentally investigated by microfocused scanning Mandelstam-Brillouin spectroscopy [18]. Fig. 1, $b, c$ shows the results of calculating the intensity and distribution of the magnetization component $m_z$ of the SW beams at the time $t = 81$ ns after the microwave signal with the frequency of $f = 5.6$ GHz was applied to the input transducers $2-5$. The simulation was carried out for the unit cell size $2 \times 2 \times 0.78\,\mu\mathrm{m}$. It was assumed that the amplitudes of all input signals are equal to $h_z = 5$ Oe, and the magnetic field $H = 1.5$ kOe is directed along the axis $Oy$. The SW input antennas with a length of $80\,\mu\mathrm{m}$ and a width of $20\,\mu\mathrm{m}$ are placed at the vertices of a rectangle with side sizes $a = 376\,\mu\mathrm{m}$ and $b = 337\,\mu\mathrm{m}$ at angles $\varphi = \pm 55°$ with respect to the field $H$, which ensures the propagation of wave beams of magnetostatic backward volume waves (MSBVW) at a frequency of $f = 5.6$ GHz in the form of caustics whose group velocity coincides with the direction of the diagonal. The brightness of the tone in Fig. 1, $b, c$ reflects the intensity of the SW, and the red and blue colors (in the online version) in Fig. 1, c reflect, respectively, the maxima and minima of the magnitude of $m_z$. It can be seen that the wave beams intersect at the location of the output antenna, the dimensions of which are identical to the dimensions of the input antennas.

The dependences of $m_z(t)$ from the output antenna $6$ for various combinations of the initial phases of the input signals are shown in Fig. 2, $a$. The inset shows the phase combinations of the signals on the input antennas $2, 4, 5$, where the phase „0" or „$\pi$" corresponds to the logical „0" or „1". It can be seen that the phase of the output signal coincides with the phase of most input signals. In this case, the signal from the output $6$ must be processed by a phase-sensitive detector [28].

If four input transducers are involved in the operation of the majority gate, and at the same time one of them excites the „reference" SW beam, the phase of which is always constant and equal to „0" or „$\pi$", then the phase of most input signals can be judged by exceeding the amplitude of the output signal of some threshold value $A^*$, set by the reference signal. This is explained in Fig. 2, $b$, where the dependences of $m_z(t)$ from the output $6$ are given for different combinations of phases for the four input signals. The transducer $3$ creates a „reference" SW beam, the phase of which is equal to „0", and its amplitude was $h_z = 15$ Oe,
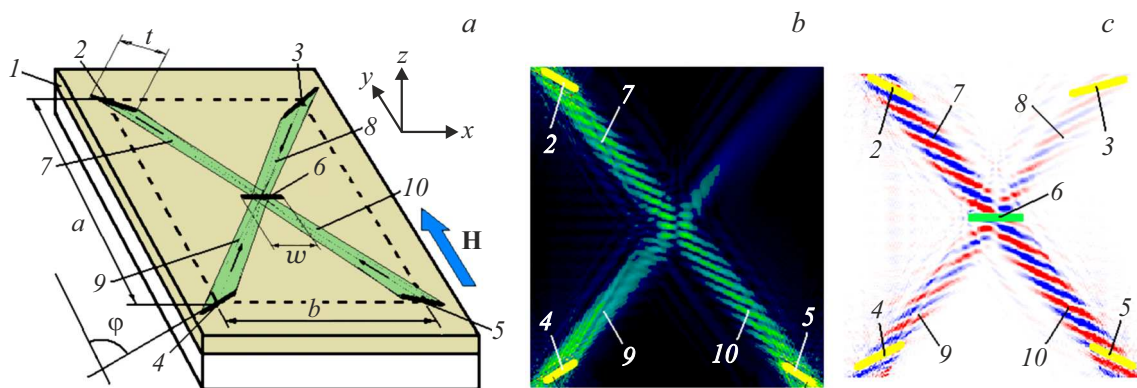
**Figure 1.** $a$ — scheme of the majority element; $b$ — intensity of SW beams excited in a $3.9\,\mu$m thick YIG film at a frequency of $f = 5.6$ GHz by input antennas *2, 4, 5* $80\,\mu$m long and $20\,\mu$m wide, located at the vertices of a rectangle with side sizes $a = 376\,\mu$m and $b = 337\,\mu$m, at angles $\varphi = \pm 55°$ with respect to the field $H = 1.5$ kOe; $c$ — distribution of $m_z$-components of microwave magnetization at a fixed time.
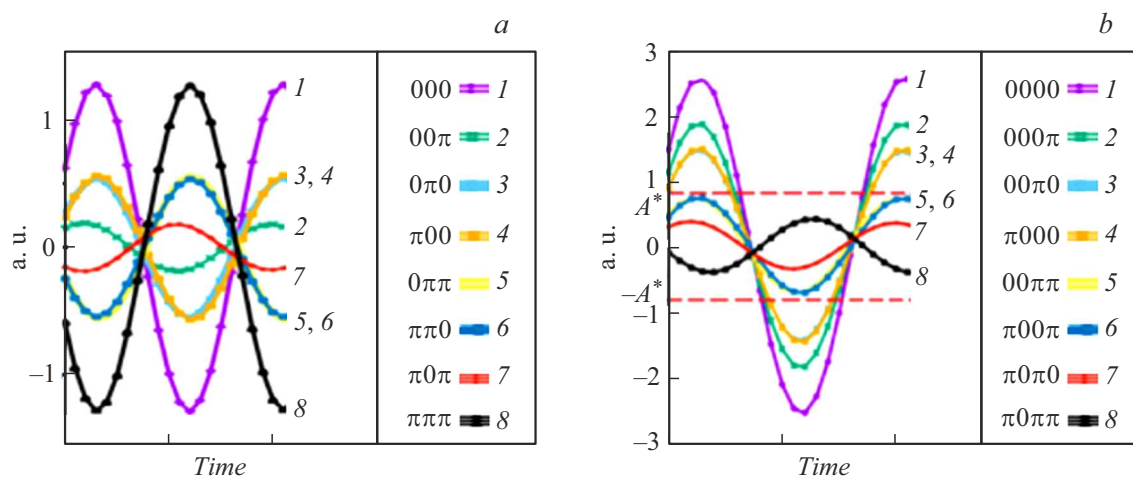


**Figure 2.** Dependences $m_z(t)$ on the output antenna in a majority gate based on a YIG film with parameters corresponding to Fig. 1, in the case of three ($a$) and four ($b$) input converters. Horizontal dotted lines show the threshold level $A^*$ for the output signal, above which the phases of most input signals coincide with the phase of the reference signal.

which is 3 times higher than the amplitudes of the signals at the other inputs. It can be seen that all signals with an amplitude above a certain level $A^*$ have a phase that coincides with the phase of the reference signal.

## 1.2. The case of YIG films of nanometer thicknesses

To show the possibility of scaling the proposed approach of constructing the logical „majority" gate. Let us consider the case of a YIG film with a thickness of $d = 50$ nm, planar dimensions of $10 \times 10\,\mu$m and with values of other parameters identical to the case discussed above. We note that the planar dimensions are set taking into account the time of micromagnetic simulation, which is directly determined by the ratio of the film dimensions and the unit cell of the numerical grid, which for this case was taken equal to $10 \times 10 \times 10$ nm. Figures 3 and 4 show

the results of micromagnetic simulation of the majority gate based on wave beams of the exchange dominated SW ($\lambda \approx 330-210$ nm) propagating at a frequency of $f = 7$ GHz. The chosen frequency is greater than the frequency $f_s = \gamma(H + 2\pi M) = 6.65$ GHz, corresponding to the short-wave limit of the spectrum of the Damon-Eshbach dipole magnetostatic surface wave (MSSW).

As the first step, the parameters of the input transducers of the SW and their position on the YIG surface were determined, at which caustics or focused wave beams converging to the center of the film are formed. For this purpose, similar to the studies [18,32], the wave field from a point source (an elementary cell of the numerical grid) placed in the center of the film was calculated for the selected frequency $f = 7$ GHz. To reduce the effect of reflections from the film edges, the losses in the YIG outside the circle with a radius of $4\,\mu$m were set increasing linearly from the values of $\alpha = 0.001$ to 1. Fig. $3, a$ shows the
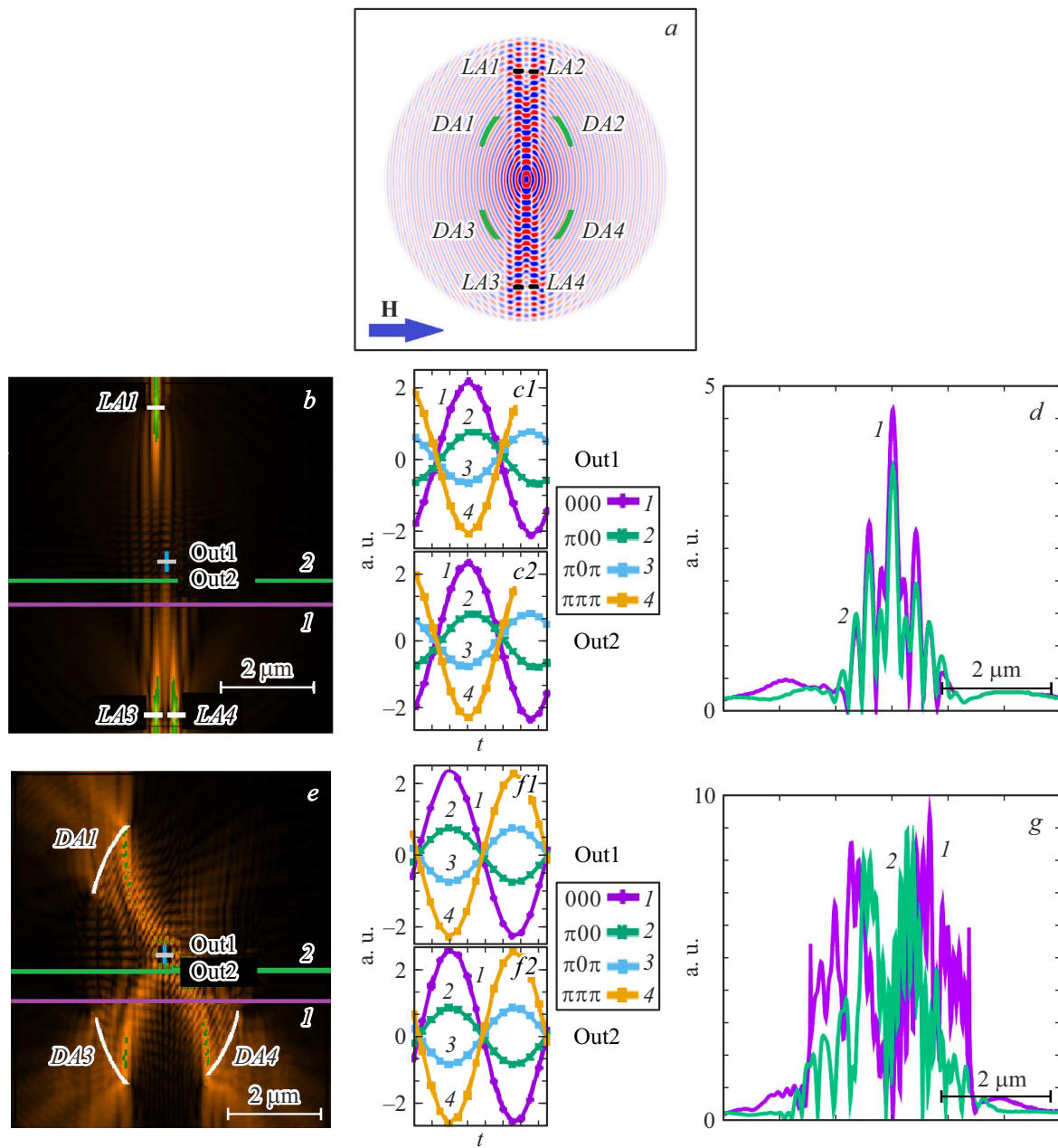
**Figure 3.** *a* — distribution of $m_z(x, y)$ at a fixed time in a 50 nm thick YIG film with planar dimensions of $10 \times 10 \,\mu m$ when excited by a point source at a frequency of $f = 7\,$GHz. The designations *LA1−LA4* and *DA1−DA4* correspond to rectilinear and arched antennas, respectively; *b, e* — distribution of the intensity of SW beams in the „majority" gate using these antennas; *c1, c2, f1, f2* — dependencies $m_z(t)$ on the output antenna Out1 and Out2 in the majority gate corresponding to Fig. *b* or *e* respectively; *d, g* — profiles of wave beams in cross sections *1* (green line (in online version)) and *2* ((purple line (in online version)), shown in Fig. *b* and *e*.

results of calculating the wave field from a point source at time $t = 10\,$ns after the start of excitation. Because of the exchange interaction the character of the isofrequency lines $f(k_x, k_y) = $ const becomes significantly different from the case of predominantly dipole SW [33]. As a result, at a frequency of $f = 7\,$GHz, SW can propagate in the film both perpendicular (geometry of MSSW with a wavelength of $\lambda \approx 310\,$nm) and along the magnetic field c $\lambda \approx 220\,$nm. In this case, the wavefront of the point source in the considered case is basically close to an ellipsoidal shape. At the same

time, from Fig. 3, *a* it can be seen that there are several pronounced rays in the wave field, in directions close to the direction of the axis $Oy$, which can be identified with the caustics of SW. At the same time, their formation in the case under consideration is apparently influenced by the saddle-type nonuniform ground state of the film due to the demagnetization fields [34].

Taking into account the above, two types of input transducers were considered for simulation the „majority" gate based on a film with selected parameters with a
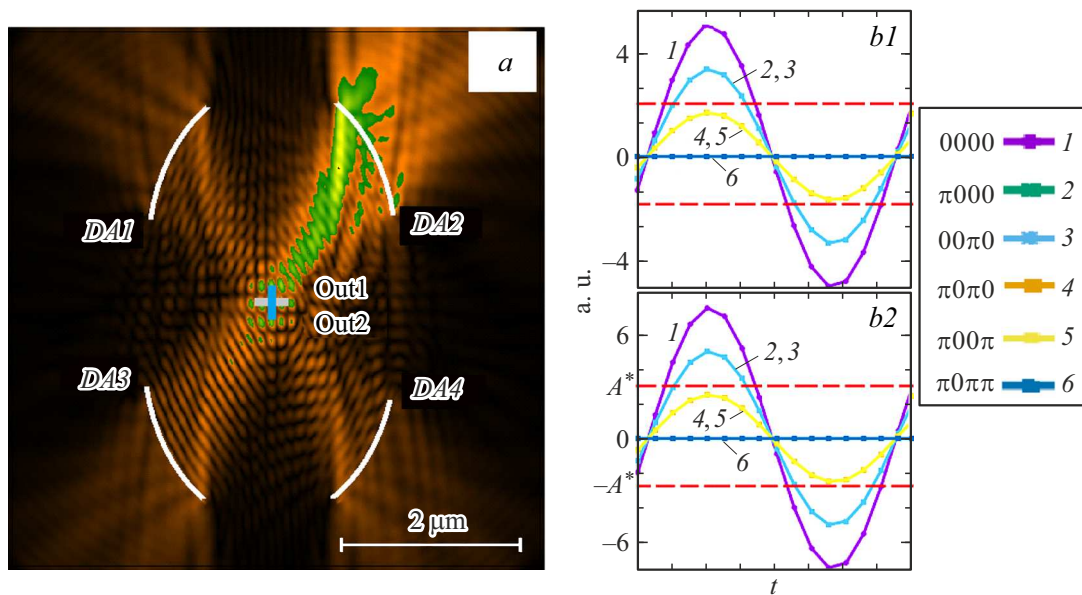
**Figure 4.** $a$ — distribution of the wave beams intensity in the „majority" gate using a reference signal from the antenna $DA2$ with an initial phase „0" and an amplitude $h_z = 0.3$ Oe. All other parameters correspond to Fig. 3, $e$; $b1, b2$ — dependencies $m_z(t)$ on the output antenna Out1 and Out2, respectively, in the majority gate using the reference signal ($a$).

magnetic field $H = 1.5$ kOe directed along the axis $Ox$, and $f = 7$ GHz. As the first, rectilinear antennas ($LA1-LA4$) with a length of 140 nm and a width of 10 nm were taken, located at the vertices of a rectangle with dimensions $a = 6400$ nm, $b = 500$ nm and oriented parallel to the wave front of the SW in rays directed along the $Oy$ axis, which at the selected points turned out to be almost parallel to the $Ox$ axis (Fig. 3, $a$). The antennas of the second type were taken to coincide in shape with part of the ellipsoidal wavefront, and had an arched shape ($DA1-DA4$) (Fig. 3, $a$). The antennas $DA$ with an aperture of 1500 nm and a width of 10 nm were located at the vertices of a rectangle with dimensions $a = 3300$ nm and $b = 2200$ nm. At the same time, it was expected that the arched shape of the input antennas $DA$ would excite focused wave beams converging in the center of the film, where the output antenna was placed. It was believed that the output antenna with a length of 140 nm and a width of 10 nm can be oriented both along the axis $Ox$ (Out1), and along the axis $Oy$ (Out2).

Fig. 3, $b, e$ shows intensity maps of SW beams excited, by the signa with a frequency of $f = 7$ GHz and an amplitude of $h_z = 0.1$ Oe at the input rectilinear ($LA1, LA3, LA4$) and arched ($DA1, DA3, DA4$) antennas, respectively. Dependencies $m_z(t)$ from the output antenna oriented along the axis $Ox$ (Out1) or the axis $Oy$ (Out2), in Fig. 3, $c1, c2, f1, f2$ correspond to the majority gates in Fig. 3, $b, e$. It can be seen that in both cases the phase of the output signal coincides with the phase of the majority on the input antennas. From comparing the amplitudes of $m_z(t)$ in Fig. 3, $c, f$, it follows that in the case of the majority gate with linear antennas ($LA$), the orientation of the output converter has little effect on the amplitude of the output signal. On the contrary, for interference of the wave beams excited

by arched antennas ($DA$), the orientation of the receiving antenna perpendicular to the direction of the magnetic field is preferable.

The spatial distribution of the intensity of the wave beams for the considered majority gates is characterized by Fig. 3, $d$ and $g$, where the profiles of the wave beams are prsented for the sections $1$ and $2$, the position of which is shown by the corresponding horizontal lines in Fig. 3, $b, e$. It can be seen that the wave beams retain their shape during propagation and are spatially limited.

Fig. 4 shows the results of micromagnetic simulation of the „majority" gate based on arched focusing transducers $DA$ on the surface of a 50 nm a thick YIG film using a reference signal. Calculations were performed for the case when the input antennas $DA1$, $DA3$, $DA4$ have signals with a phase „0" or „π" and the same amplitude $h_z = 0.1$ Oe,and a reference signal with amplitude $h_z = 0.3$ Oe and phase „0"is applied to the antenna $DA2$. Fig. 4, $b1, b2$ shows the dependencies of $m_z(t)$ with the output antenna oriented along the axis $Ox$ (Out1) and the axis $Oy$ (Out2) respectively. It can be seen that the orientation of the output antenna along the aperture of the input transducers increases the output signal by 1.5 times.

## 1.3. Permalloy film case

It is also of interest to consider the applicability of the proposed approach for the case of ferromagnetic metal films, since they are easier to combine with the CMOS technologies used in comparison with the YIG films. Fig. 5 shows the results of micromagnetic simulation of the logical majority gate using a reference signal based on SW caustics in permalloy film (Py) with dimensions
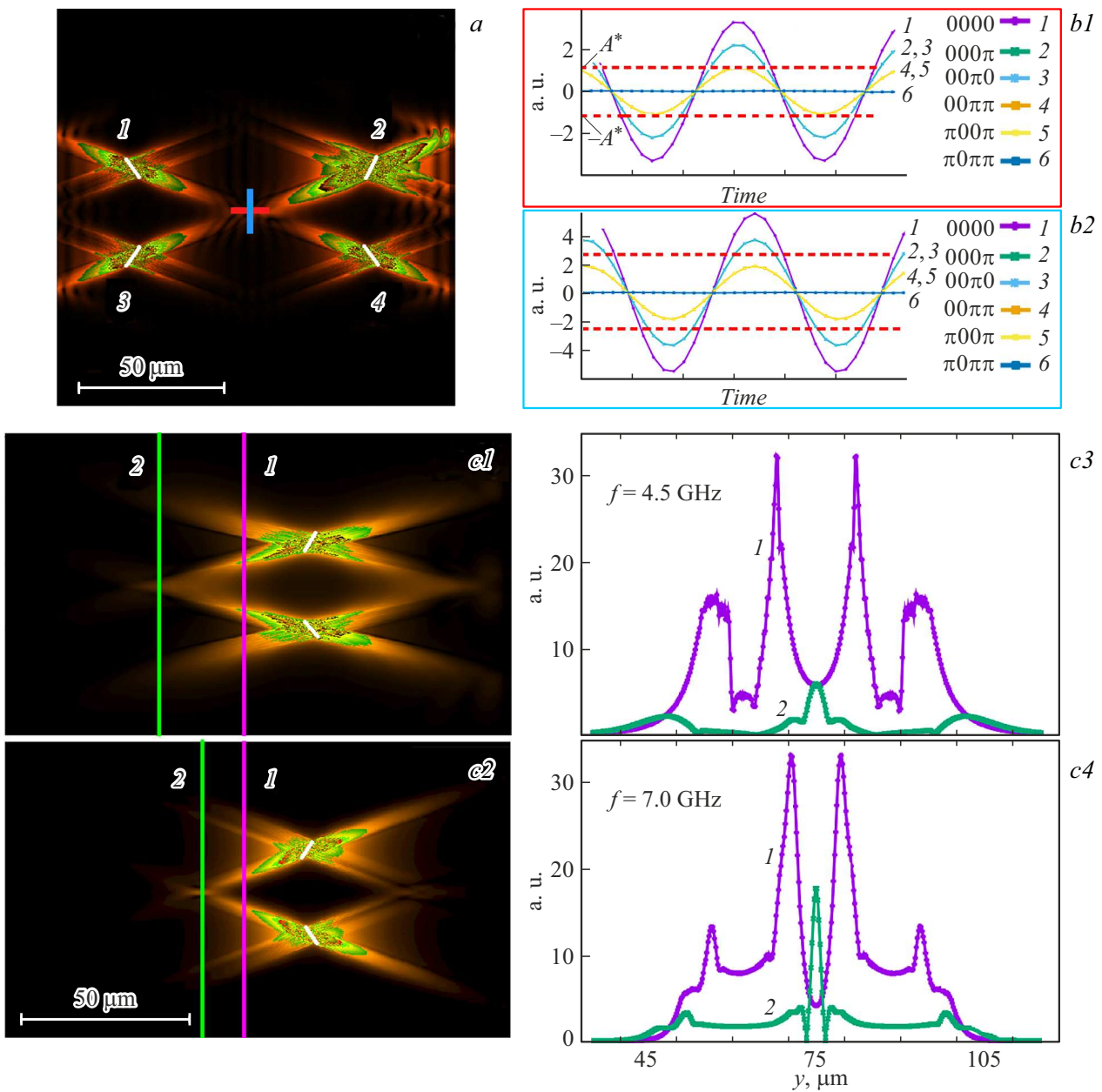
**Figure 5.** Results of micromagnetic simulation of the majority gate based on permalloy film. $a$ — intensity distribution of wave beams in the majority based on interference with the SW frequency $f = 6$ GHz excited by antennas *1, 3, 4* with the „reference" wave excited by the input antenna *2*; *b1, b2* — dependencies $m_z(t)$ on the output antenna for various combinations of the initial phases of input signals when the output antenna is oriented perpendicular and parallel to the direction of the field $H$, respectively; $c$ — dependence on frequency dependence of the position of the intersection point of the wave beams (shown by the vertical green line *2*) and the distribution of the intensity of the wave beams along the sections *1* and *2* passing near the input antennas (vertical purple line *1*) and through the intersection point of the wave beams; *c1, c3* — correspond to the frequency $f = 4.5$ GHz, for Fig. *c2, c4*, $f = 7$ GHz.

$150 \times 150 \times 0.1 \, \mu$m. The magnetic parameters were taken to be $4\pi M = 10807$ G, $\alpha = 10^{-2}$, $A = 13 \cdot 10^{-12}$ J/m. The magnetic field $H = 150$ Oe is directed along the axis $Oy$. The unit cell size was $200 \times 200 \times 20$ nm. The input antennas with a length of $10 \, \mu$m and a width of $1 \, \mu$m are placed at the vertices of the rectangle $30 \times 80 \, \mu$m at an angle of $\varphi = \pm 35°$ with respect to the field $H$. It was believed that the input antennas received a signal at

a frequency of $f = 6$ GHz, corresponding to the frequency band of the MSSW. The amplitude of the exciting field $h_z$ on the antennas *1, 3, 4* was equal to 0.1 Oe, and the initial phases took the values „0" or „$\pi$". A reference signal with phase „0" and amplitude $h_z = 0.3$ Oe was applied to antenna $\hat{2}$. The output antenna of the same length and width as the input antenna was located in the center of the film and was oriented either along the $Ox$ axis or along $Oy$.

Fig. 5, $b1, b2$ shows the dependencies of $m_z(t)$ of the output signals when the output antenna is oriented perpendicular or parallel to the $H$ field, respectively. It can be seen that the output signals with an amplitude above the threshold level of $A^*$ have a phase that coincides with the phase of the reference signal. Comparison of signal amplitudes in Fig. 5, $b1$ and $b2$ shows that the output signal is noticeably larger in the case when the overlap of the apertures of the input and output transducers is maximum. Fig. 5, $c$, using the example of two input antennas, illustrates the spatial distribution of the intensity of wave beams as a function of the frequency. It can be seen that the wave beams are spatially well confined. At the intersection of the caustics, the beam width at the level of 1/2 does not exceed $5 \mu$m, which in this case is less than the aperture of the receiving antenna (Fig. 5, $c3, c4$). From a comparison of the results in Fig. 5, $c1$ and $c2$, it can be seen that the intersection point of the SW caustics, which can be considered as the focus position for the optical system formed by the input antennas, shifts towards the input antennas as the frequency increases. This behavior of the focus reflects the chromatic aberration of the focusing transducers MSSW in tangentially magnetized films [15–18]. Note also that the shift of focus to the input antennas is accompanied by an increase in the signal amplitude at the intersection of the caustics (Fig. 5, $c3, c4$).

## Conclusion

Thus, the propagation and interference of spin waves caustics in the YIG films and permalloy are considered using the micromagnetic simulation. It is shown that the logical „majority“ gate can be implemented based on the effects of interference of caustics and focused wave beams of SW. A feature of the proposed approach to the construction of the majority gate is the equal distance of all input antennas for spin waves from the output converter, which potentially eliminates the need to use attenuators to equalize the amplitudes of SW interfering on the output antenna. In addition, it is shown that the use of an additional reference signal with a fixed phase („0“ or „$\pi$“) and an amplitude 3 times higher than the amplitude of the information signals, allows to convert the phase of the output signal of the „majority “ gate into an amplitude. This conversion method promises a more convenient reading of the magnetic phase than the previously proposed approach due to local non-adiabatic parallel parametric pumping [26].

We add that from the point of view of the implementation of the proposed approach, it is necessary to take into account that the receiving converter located in the caustic intersection area should have supply lines and contact pads for connecting microprobes. It is clear that these sections of the output antenna for the SW will receive peripheral parts of the caustics, which will make a parasitic contribution to the result of interference on the receiving antenna. We believe that it is possible to reduce the contribution of peripheral caustic regions to the total signal using the approach proposed in [35] by making the width of the supply lines significantly larger than both the width of the receiving antenna and the length of the $\lambda$ spin wave.

## Funding

## Conflict of interest

The authors declare that they have no conflict of interest.

## References

[1] A. Khitun, M. Bao, K.L. Wang. J. Phys. D: Appl. Phys., **43** (26), 264005 (2010).
DOI: 10.1088/0022-3727/43/26/264005

[2] A. Mahmoud, F. Ciubotaru, F. Vanderveken, A.V. Chumak, S. Hamdaoui, C. Adelmann, S. Cotofana. J. Appl. Phys., **128** (16), 161101 (2020). DOI: 10.1063/5.0019328

[3] A. Kozhevnikov, F. Gertz, G. Dudko, Y. Filimonov, A. Khitun. Appl. Phys. Lett., **106** (14), 142409 (2015).
DOI: 10.1063/1.4917507

[4] Y. Khivintsev, M. Ranjbar, D. Gutierrez, H. Chiang, A. Kozhevnikov, Y. Filimonov, A. Khitun. J. Appl. Phys., **120** (12), 123901 (2016). DOI: 10.1063/1.4962740

[5] M. Balinsky, D. Gutierrez, H. Chiang, A. Kozhevnikov, G. Dudko, Y. Filimonov, A.A. Balandin, A. Khitun. Scientific Reports, **7**, 11539 (2017).

[6] Yu.V. Khivintsev, A.V. Kozhevnikov, V.K. Sakharov, G.M. Dudko, Yu.A. Filimonov, A. Khitun. ZhTF, **89** (11), 1712 (2019) (in Russian).
DOI: 10.21883/JTF.2019.11.48333.118-19

[7] M. Balynsky, A. Kozhevnikov, Y. Khivintsev, T. Bhowmick, D. Gutierrez, H. Chiang, G. Dudko, Y. Filimonov, G. Liu, C. Jiang, A.A. Balandin, R.E. Lake, A. Khitun. J. Appl. Phys., **121** (2), 024504 (2017). DOI: 10.1063/1.4973115

[8] B. Heinz, T. Brächer, M. Schneider, Q. Wang, B. Lägel, A.M. Friedel, D. Breitbach, S. Steinert, T. Meyer, M. Kewenig, C. Dubs, P. Pirro, A.V. Chumak. Nano Lett., **20** (6), 4220 (2020). DOI: 10.1021/acs.nanolett.0c00657

[9] Y.V. Khivintsev, A.V. Kozhevnikov, G.M. Dudko, V.K. Sakharov, Y.A. Filimonov, A.G. Khitun. Phys. Metals and Metallography, **120** (13), 76 (2019).
DOI: 10.18500/1817-3020-2021-21-3-249-263

[10] Q. Wang, M. Kewenig, M. Schneider, R. Verba, F. Kohl, B. Heinz, M. Geilen, M. Mohseni, B. Lägel, F. Ciubotaru, C. Adelmann, C. Dubs, S.D. Cotofana, O.V. Dobrovolskiy, T. Brächer, P. Pirro, A.V. Chumak. Nature Electron., **3**, 765 (2020). DOI: 10.48550/arXiv.1905.12353

[11] A.V. Sadovnikov, C.S. Davies, S.V. Grishin, V.V. Kruglyak, D.V. Romanenko, Yu.P. Sharaevskii, S.A. Nikitov. Appl. Phys. Lett., **106** (19), 192406 (2015). DOI: 10.1063/1.4921206

[12] Q. Wang, B. Heinz, R. Verba, M. Kewenig, P. Pirro, M. Schneider, T. Meyer, B. Lägel, C. Dubs, T. Brächer, A.V. Chumak. Phys. Rev. Lett., **122**, 247202 (2019).
DOI: 10.1103/PhysRevLett.122.247202

[13] Y.V. Khivintsev, V.K. Sakharov, A.V. Kozhevnikov, G.M. Dudko, Y.A. Filimonov, A. Khitun. J. Magn. Magn. Mater., **545**, 168754 (2022).
DOI: 10.1016j.jmmm.2021.168754

[14] G.M. Dudko, A.V. Kozhevnikov, Yu.V. Khivintsev, Yu.A. Filimonov, A.G. Khitun, S.A. Nikitov. Radiotekhnika i elektronika, **63**, (10), 1105 (2018) (in Russian).
DOI: 10.1134 S0033849418100091

[15] A.V. Vashkovsky, A.V. Stalmakhov, D.G. Shakhnazaryan. Izvestiya Vuzov. (in Russian) Phizika, **31** (11), 67 (1988) (in Russian).

[16] E.G. Locke. Radiotekhnika i elektronika, **60** (1), 102 (2015). (in Russian). DOI: 10.7868 S0033849415010106

[17] A.Yu. Annenkov, S.V. Gerus, E.H. Lock. Europhys. Lett., **123** (4), 44003 (2018). DOI: 10.1209/0295-5075/123/44003

[18] M. Madami, Y. Khivintsev, G. Gubbiotti, G. Dudko, A. Kozhevnikov, V. Sakharov, A. Stal′makhov, A. Khitun, Y. Filimonov. Appl. Phys. Lett., **113** (15), 152403 (2018). DOI: 10.1063 1.5050347

[19] D. Hampel, R.O. Winder. IEEE Spectr., **8** (5), 32 (1971).

[20] A. Khitun, K.L. Wang. J. Appl. Phys., **110** (3), 034306 (2011). DOI: 10.1063/1.3609062

[21] A. Khitun, M. Bao, K.L. Wang. IEEE Trans. Magn., **44** (9), 2141 (2008). DOI: 10.1109/TMAG.2008.2000812

[22] A. Khitun. J. Appl.Phys., **111** (5), 054307 (2012). DOI: 10.1063/1.3689011

[23] S. Klingler, P. Pirro, T. Brächer, B. Leven, B. Hillebrands, A.V. Chumak. Appl. Phys. Lett., **105** (15), 152410 (2014). DOI: 10.1063/1.4898042

[24] S. Klingler, P. Pirro, T. Brächer, B. Leven, B. Hillebrands, A.V. Chumak. Appl. Phys. Lett., **106** (21), 212406 (2015). DOI: 10.1063/1.4921850

[25] A. Mahmoud, F. Vanderveken, C. Adelmann, F. Ciubotaru, S. Hamdioui, S. Cotofana. AIP Adv., **10** (3), 035119 (2020). DOI: 10.1063/1.5134690

[26] T. Brächer, F. Heussner, P. Pirro, T. Meyer, T. Fischer, M. Geilen, B. Heinz, B. Lägel, A.A. Serga, B. Hillebrands. Sci. Rep., **6**, 38235 (2016). DOI: 10.1038/srep38235

[27] N. Kanazawa, T. Goto, K. Sekiguchi, A.B. Granovsky, C.A. Ross, H. Takagi, Y. Nakamura, H. Uchida, M. Inoue. Sci. Rep., **7**, 7898 (2017). DOI: 10.1038/s41598-017-08114-7

[28] T. Fischer, M. Kewenig, D.A. Bozhko, A.A. Serga, I.I. Syvorotka, F. Ciubotaru, C. Adelmann, B. Hillebrands, A.V. Chumak. Appl. Phys. Lett., **110** (15), 152401 (2017). DOI: 10.1063/1.4979840

[29] G. Talmelli, T. Devolder, N. Träger, J. Förster, S. Wintz, M. Weigand, H. Stoll, M. Heyns, G. Schütz, I.P. Radu, J. Gräfe, F. Ciubotaru, C. Adelmann. Sci. Adv., **6** (51), abb4042 (2020). DOI: 10.1126/sciadv.abb4042

[30] M.J. Donahue, D.G. Porter. *OOMMF user's Guide. Interagency Report* (NIST 6376, 1999).
DOI: 10.6028/NIST.IR.6376

[31] M. Dvornik, Y.Au, V. Kruglyak, *in Magnonics, Topics in Applied Physics, ed. by S.O. Demokritov, A.N. Slavin* (Springer-Berlin, Heidelberg, 2013), v. 125, p. 101.

[32] G.M. Dudko, A.V. Kozhevnikov, V.K. Sakharov, A.V. Stalmakhov, Yu.A. Filimonov, Yu.V. Khivintsev. Izvestia Sarat. un-ta. Novaya Seriya. (in Russian). Series: Fizika, **18** (2), 92 (2018). (in Russian).
DOI: 10.18500/1817-3020-2018-18-2-92-102

[33] V. Veerakumar, R.E. Camley. Phys. Rev. B, **74** (21), 214401 (2006). DOI: 10.1103/PhysRevB.74.214401

[34] V.G. Shavrov, V.I. Shcheglov. *Magnitostatisticheskie volny v neodnorodnykh polyakh.* (Fizmatlit, M., 2016), (in Russian).
DOI: 10.1201 9781003046226

[35] P. Gruszecki, M. Kasprzak, A.E. Serebryannikov, M. Krawczyk, W. Śmigaj. Sci. Rep., **6**, 22367 (2016).
DOI: 10.1038/srep22367